

**CONSTRAINTS ON TESSERA COMPOSITION FROM MODELING OF TELLUS REGIO, VENUS.** M. S. Gilmore<sup>1</sup>, P. G. Resor<sup>1</sup>, R. Ghent<sup>2</sup>, D. A. Senske<sup>3</sup>, R. R. Herrick<sup>4</sup> <sup>1</sup>Dept. of Earth and Environmental Sciences, Wesleyan University, Middletown CT, 06459, mgilmore@wesleyan.edu, <sup>2</sup>Univ. of Toronto, <sup>3</sup>JPL, <sup>4</sup>University of Alaska Fairbanks.

**Introduction:** The heavily deformed Venus tessera terrain is generally embayed by volcanic plains materials that cover the majority of the surface [1]. The tesserae thus provide the best chance to access rocks that are derived from the early history of the planet, an era for which we currently have little information, but may have been more water-rich [e.g., 2]. Goals of this study are to perform high resolution (~100 m/pixel) mapping of a specific tessera highland, Tellus Regio, and determine the type, stratigraphy and wavelength of structures. These parameters are then input into a linearized model in order to estimate lithospheric properties of this highland through time.

**Geomorphic Mapping:** Four units are visible in the SW margin of Tellus, where a fold belt (Fig. 1, B) consisting of recognizable plains materials lies between 3 tessera units (Fig. 1, A, C, D). NW-trending ridges and overlying NE-trending graben are present in the fold belt and adjacent tessera units (units A and C) and are attributed to contemporaneous compressional deformation. The NW-trending ridges differ morphologically from older fabrics preserved in the 3 regions of tessera terrain. These observations support the hypotheses that 1) tessera fabrics can form under distinct strain histories, and that 2) SW Tellus was formed by the assembly of these preexisting fabrics and intervening volcanic plains during a collisional event.

**Structural Wavelengths:** Ridge crests were mapped by examining Magellan Cycle 1 and Cycle 3 left-looking image pairs and correlating these data to SAR characteristics typical of ridges (e.g., sinuous planform, gradual brightness changes across the ridge). Ridge wavelengths were computed in ArcGIS by measuring distances between nearest mapped ridge crests at 10s of points along each ridge (dots in Fig. 1).

Mean fold wavelengths of the tessera interior, indenter and western margin are ~13 km (Fig. 1 C, A, E). The wavelengths measured here (n=1965) are similar to those previously derived for the whole of Tellus Regio (n=23 measurements) and other tessera plateaus [3,4]. Smaller mean wavelengths of ~8 km (n=493) are recorded in the tessera of SE portion of Fig. 1 (area D) and for the materials of the fold belt (~5 km (n=769), area B).

**Lithosphere Modeling:** To evaluate the lithospheric properties constrained by fold wavelengths at Tellus Regio we have implemented the linearized perturbation model of [5] in Matlab<sup>®</sup> following the approach of [6]. In this model a single dominant wave-

length instability develops in response to layer-parallel strain of a relatively stiff brittle surface layer overlying a relatively soft ductile substrate [e.g., 7]. We present strength envelopes for a range of likely strain rates [e.g., 8], thermal gradients and compositions (Fig. 2). Folds with 10-15 km wavelengths as measured for the tessera units can be produced under the following conditions: • Dunite [9] and dry anorthite [10] rheologies require high thermal gradients  $\geq 40$  K/km even at low strain rates ( $10^{-17}$ /s). • Columbia diabase [11] requires strain rates ( $10^{-15}$ - $10^{-16}$ /s) and thermal gradients (25-55K/km) higher than present day Venus and consistent with previous estimates [3]. • Wet rheologies are possible. A wet gabbro [12] can deform at ( $10^{-15}$ - $10^{-16}$ /s) and lower thermal gradients ( $\leq 10$ K/km), or higher strain rates and thermal gradients. Wet anorthite [10] can deform under high strain rates. • Dry quartzite [13] is too weak to buckle. This is probably true of any quartz-rich rheology.

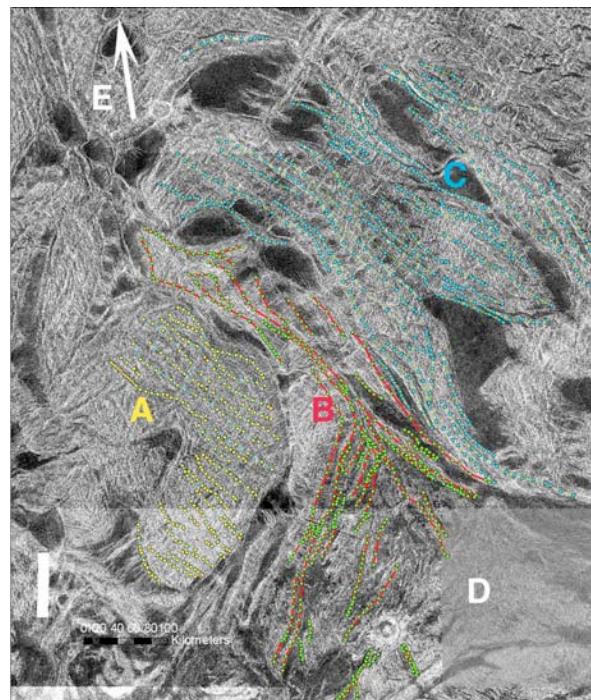


**Fig. 1.** FMAP image of SW Tellus Regio. Lines indicate ridge crests used to measure structural wavelengths. A - "Indenter", B - Fold belt, C - Plateau interior, D - SE geomorphologic unit, E - to the western margin. Image subtends ~28-35°N, 75-81°E; north is up.

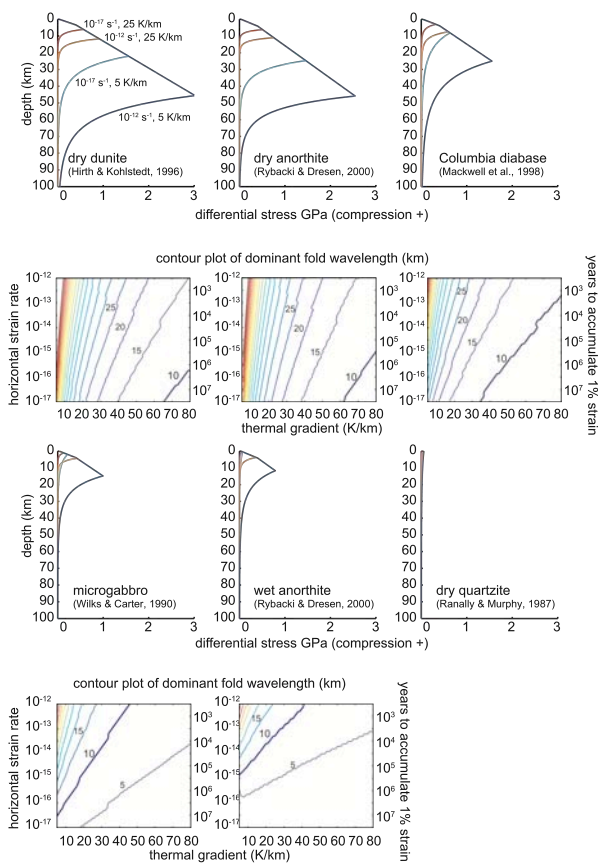


**Figure 2. Strength envelopes and fold wavelengths for varying composition, strain rate, and thermal gradient.**

**Shortening estimates** for the fold belt were calculated by comparing the total length along a topographic profile to distance on the surface using topography generated from Magellan Cycle 1 and Cycle 3 left-looking stereopairs [6]. A minimum shortening is derived by assuming that the plate is buckling with no internal deformation. This yields shortening values of <1%, similar to that estimated for folds in Ovda Regio [4]. We note that high thermal gradients and high surface temperatures may permit significant distributed strain that is not reflected in the fold measurements. Surface-breaking thrust faults would also lead to unaccounted strain [e.g., 15].

**Discussion:** Systematic measurements of ridge wavelengths across SW Tellus Regio yield values that are similar over large portions of the area, consistent with similar lithospheric properties across this region. An exception to this is the folds and troughs of the tessera unit in the SE corner of Fig. 1, which record structures of a different wavelength and orientation than the remainder, implying a unique strain history or lithospheric properties. The ridge belt also deforms at a shorter wavelength than the surrounding tessera re-

gions. These plains materials are perhaps more likely to comprise thinner crust, or include detachment surfaces that allow shallow deformation at shorter wavelengths. NW-trending ridges and NE-trending graben extend across 3 of the 4 mapped units lie at the same stratigraphic level and are interpreted to result from a collisional event that deformed preexisting tessera and plains materials. Thus the formation of the oldest tessera fabric predates plateau formation. SW Tellus contains a clear example of the incorporation of plains materials into this tessera plateau and requires that plains formation was occurring contemporaneously with some stages of tessera plateau formation (uplift and compression).

Wavelengths of structures ~ 10-15 km correspond to shortening <1%. Although this estimate accommodates no internal deformation, such low strain estimates may be reasonable based on low amplitude to wavelength ratios (~1:10) of the folds in Tellus Regio. These structures require elevated strain rates and thermal gradients for mafic compositions or dry anorthite. Modeling of folds using a minimum strain criterion yields thermal gradients of ~30-80 K/km for the range of observed wavelengths and reasonable strain rates [16]. These values greatly exceed ~ 5 K/km estimates for the present-day near-surface thermal gradient [e.g., 17], and exceed the 17 K/km conservative model estimate of [3] that assumed 15 km wavelength folds and 25% strain. Wet compositions require very high strain rates (and short deformation times). Quartz-rich rheologies are likely excluded. Low 1 micron emissivity values for tesserae may also need to consider felsic compositions other than quartz (e.g., anorthosite, [18]).

**References:** [1] Ivanov and Head (1996) *JGR* 101, 14861. [2] Donahue and Pollack (1983) in Venus, edited by D. M. Hunten et al., pp. 1003–1036, Univ. of Ariz. Press, Tucson. [3] Brown and Grimm (1997) *EPSL* 147, 1. [4] Ghent and Hansen (1999) *Icarus* 139, 116. [5] Fletcher and Hallet (1983) *JGR* 88, 7457. [6] Dombard and McKinnon (2001) *Icarus* 154, 321. [7] Biot (1961) *GSAB* 72, 1595. [8] Grimm (1994) *JGR* 99, 23163. [9] Hirth and Kohlstedt (1996) *EPSL* 144. [10] Rybacki & Dresen (2000) *JGR* 105, 26017. [11] Mackwell et al. (1998) *JGR* 103, 12053. [12] Wilks and Carter (1990) *Tectonophysics* 182, 57. [13] Ranally and Murphy (1987) *Tectonophysics* 132, 281. [14] Herrick et al. (2010) *LPSC* 41, #1622. [15] Romeo and Turcotte (2008) *EPSL* 276, 85. [16] Grimm (1994) *JGR* 99, 23163. [17] Smrekar and Parmentier (1996) *JGR* 101, 5397. [18] Mueller N. et al. (2008) *JGR*, 113, E00B17.

**Acknowledgement:** Support from NASA PG&G is gratefully acknowledged. Thanks to Max Gardner for help with digitizing and GIS work.